Journal of Hydrology 603 (2021) 127056

Contents lists available at ScienceDirect

Journal of Hydrology

journal homepage: www.elsevier.com/locate/jhydrol

A new approach to quantify propagation time from meteorological to hydrological drought

Sarah Ho [1], Lu Tian [1], Markus Disse, Ye Tuo [*]

Chair of Hydrology and River Basin Management, Technical University of Munich, Arcisstrasse 21, 80333 Munich, Germany

ARTICLE INFO

Keywords:
Drought
Propagation time
Hydrological drought
Standardized indices
Remote sensing

ABSTRACT

Of particular importance in a world of increasing water scarcity is the temporal and spatial relationship between a shortage in rainfall—meteorological drought—and a shortage in available water, or hydrological drought. Propagation time from meteorological to hydrological drought should be calculated at a higher (sub-monthly) temporal resolution with considerations for spatial expansion. A new framework for propagation time calculation from one index to another is established that uses the run theory, high-resolution remote sensing data on a daily time step. The framework is demonstrated using standardized drought indices representing precipitation, runoff, evapotranspiration, and soil moisture in the Central Asian subcontinent to measure the temporal shift (propagation time) in affected drought area, bringing a new perspective to contemporary drought analysis. Several variables from the water cycle are chosen to provide hydrological context for different propagation times. Correlation analyses for propagation time are shown to be ambiguous in interpretation and precision when compared to the temporal shift, which is clearly defined and calculated on a daily time step. Moreover, the results of temporal shift analyses indicate that deficits in evapotranspiration and runoff can precede deficits in precipitation, while soil moisture deficit almost always follows, highlighting the effects of additional influencing factors aside from precipitation on types of hydrological drought. While it is limited by current understanding of drought definition techniques, availability and quality of remote sensing products, and selection of characteristics for observation, use of the temporal shift over the correlation analysis provides a sub-monthly estimate of drought propagation time that may prove useful for detailed analyses, particularly in rapidly developing flash drought events.

1. Introduction

Drought is commonly understood as a shortage of water for an extended duration. However, despite decades of research, there are still many questions about what precisely should be considered “drought”. Scientists have studied drought primarily through drought indices that attempt to quantify degrees of drought using different observed variables and calculation methods, which are usually defined in three dimensions: space, time, and intensity. Drought can be classified based on impact as meteorological, hydrological, agricultural, or socioeconomic drought (Hao and Singh, 2015; Zargar et al, 2011). More recent drought classification types include flash drought, commonly understood as a rapid intensification of dryness due to increased evapotranspiration resulting in drought (Lisonbee et al., 2021; Otkin et al., 2018; Pendergrass et al., 2020)—and ecological drought (Crausbay et al., 2017), which describes water deficits that affect ecosystem functions and services in the environment. Meteorological drought indices can be only reliant on precipitation, such as in the Standardized Precipitation Index (SPI) (McKee et al., 1993), while other meteorological indices—such as the modified SPI variant, the Standard Precipitation and Evapotranspiration Index (SPEI) (Beguería et al., 2014), and the Palmer Drought Severity Index (PDSI) (Palmer, 1965)—can include the effects of evapotranspiration using temperature inputs (Mishra and Singh, 2010; Zargar et al., 2011). Hydrological drought broadly describes shortages in surface and subsurface water (Van Loon, 2015), such as water levels in lakes and discharge in rivers. This could include soil moisture, which—depending on the researcher—is also considered an agricultural drought indicator (Mishra and Singh, 2010; Van Loon, 2015; Zargar et al., 2011). It is generally assumed that these different types of drought can affect each other, but that ultimately, meteorological drought is

* Corresponding author.
E-mail address: ye.tuo@tum.de (Y. Tuo).
[1] These authors contributed equally to this work.

https://doi.org/10.1016/j.jhydrol.2021.127056

Available online 15 October 2021

considered the driving force (Van Loon, 2015; Zargar et al., 2011).

Many contemporary studies seek to understand how types of droughts move from one to the other (Guo et al., 2020; Huang et al., 2017; Jehanzaib et al., 2019; Orth and Destouni, 2018; Wang et al., 2016; Xu et al., 2019), with particular importance on spatio-temporal characteristics (Guo et al., 2018a; Guo et al., 2018b; Mishra and Singh, 2011; Orth and Destouni, 2018). One such improvement is the need to identify the propagation time, or the amount of time it takes for effects of a drought event to appear in a different type of drought. The successful management of water resources in the impending climate change crisis demands improvement in prediction and identification of hydrological extreme events such as floods and droughts, making an understanding of this propagation from meteorological to hydrological drought a critical priority.

Model-based analyses of drought propagation have been attempted on the catchment scale (Tallaksen et al., 2009; Van Loon et al., 2012). While useful, such catchment-scale studies are restrained by local influencing factors like topography and are therefore limited in their ability for generalization: continental- and sub-continental studies are therefore necessary to understand propagation mechanics and trends in an increasingly warmer world. Large study regions pose new problems—the broad range of catchment types in a continental-scale region mean that potential models must be selected with care to ensure representation of key processes (Trambauer et al., 2013). However, many regions of the world have insufficient data to support such detailed, physically- or semi-physically based models, especially in low flow regions, making it necessary to investigate statistical methods for identifying drought (Van Loon, 2015).

Current approaches to approximate propagation time generally involve a correlation analysis between two indices calculated at different time scales. Correlations have previously been calculated between indices for comparative analyses (Mishra and Singh, 2010; Narasimhan and Srinivasan, 2005; Shukla and Wood, 2008), but Barker et al. (2016) were among the first to explicitly use it as a method to calculate propagation time. Since then, their claim of a connection between correlated time scales and propagation time have been used in several studies (Gevaert et al., 2018; Huang et al., 2017; Jehanzaib et al., 2019; Wu et al., 2021; Xu et al., 2019), though the interpretation of this relation—in other words, the derivation of the approximate propagation time from the highest correlated time scales—is still unclear. For example, Barker et al. (2016) mention that it "provides an indication of the time", where "the SPI accumulation period with the strongest correlation with [the standardized streamflow index of one month] SSI-1… was used as an indicator for drought propagation". It is unclear how this indicator should be understood if the hydrological index time scale is not 1 month—studies using this connection do not provide detailed interpretation or analysis of it (Huang et al., 2017; Wu et al., 2018; Xu et al., 2019). Correlation analyses also lack the ability to describe characteristics of drought such as spatial extent, onset, and peak. Moreover, their application in large study areas is limited: the correlation between precipitation and streamflow at an outlet may provide an idea of the relationship between those variables but does not describe the spatial variability within that region. A comparison of three propagation time techniques (the correlation method, a run theory method, and a non-linear response method) by Wu et al. (2021) shows that there is little concurrence between results from current methods, indicating that further development and innovation in this field is necessary.

There have been few, if any, attempts to calculate propagation time with higher (sub-monthly) precision, which would improve understanding of drought development and recovery. Time series analyses for this are possible (Mishra and Singh, 2011), but the success of such studies is, as in most fields of hydrology, limited by observed data: the widespread availability of coarser monthly data results in analyses that lack precision on a sub-monthly scale. While such a scale might be relevant for multi-year, slowly-developing drought events, the recent recognition of rapidly developing flash drought events will require sub-monthly analyses, ideally daily, to sufficiently describe these processes (Otkin et al., 2018; Pendergrass et al., 2020). Recent advances in remote sensing technology have enabled analysis of hydrological processes in increasingly finer temporal and spatial resolution, particularly in low data catchments across the globe, but these high-resolution products have not yet been applied for drought propagation time.

Calculation of propagation time from meteorological to hydrological drought also remains complex due to the multivariate nature of drought. Many researchers have discussed the inability of any single index to properly capture drought (Hao and AghaKouchak, 2013; Hao and Singh, 2015; Li et al., 2017; Rajsekhar et al., 2015; Wang et al., 2016). Streamflow and runoff are commonly used as hydrologic indices (Barker et al., 2016; Mishra and Singh, 2010; Shukla and Wood, 2008; Van Loon, 2015; Zargar et al., 2011); however, other hydrological variables in conjunction with precipitation can provide more insight into changes in runoff (Hao and AghaKouchak, 2013; Hao and Singh, 2015; Rajsekhar et al., 2015). Precedent soil moisture conditions are a strong indicator for runoff (Van Loon, 2015); likewise, evapotranspiration can greatly affect soil moisture conditions (Otkin et al., 2018; Pendergrass et al., 2020; Van Loon, 2015) and is often monitored alongside precipitation via indices like SPI and SPEI (Bayissa et al., 2018; Beguería et al., 2014; Nicolai-Shaw et al., 2017; Spinoni et al., 2019; Zargar et al., 2011; Zhu et al., 2016). Thus, soil moisture and evapotranspiration have been included in multivariate studies for their relevance in the hydrologic cycle (Keyantash and Dracup, 2004; Li et al., 2017; Nicolai-Shaw et al., 2017). Because drought is multivariate and complex, an analysis of propagation time should also be multivariate and complex—studying precipitation, runoff, soil moisture, and evapotranspiration in parallel could provide hydrological context for propagation time.

Water resources management decisions are influenced by the availability and monitoring of surface water, which is a primary victim of hydrological drought (Van Loon, 2015; Van Loon and Van Lanen, 2012; Wang et al., 2016). Proper responses to hydrological drought propagation, however, require a holistic and multivariate approach to understand the influence factors behind propagation time. In this study, our objectives are twofold: first, to establish a new framework for investigating propagation time from meteorological to hydrological drought to overcome the limitations of the correlation method; and second, to compare the new methods with previously established methods for further understanding of the relationship between highest correlated drought time scales. We use one drought index representing meteorological drought and three drought indices reflecting hydrological drought to contextualize the reasons behind different propagation times. These objectives are part of a larger effort to understand spatial and temporal drought propagation.

2. Methodology

2.1. Study area – Central Asia

The study area, Central Asia (Fig. 1), is an arid to semi-arid sub-continental region consisting of countries—specifically Kazakhstan, Uzbekistan, Kyrgyzstan, Turkmenistan, Tajikistan, and the Xinjiang province in northwest China—with strong dependencies on agriculture. Precipitation in this region is dominated by snow in the higher mountainous regions in the winter, while hot and dry conditions prevail in the summer. Drought conditions occur regularly and can stretch across the entire region with aggravated effects from poor water distribution, desertification, salinization, and unsustainable land use practices (Patrick, 2017). Stream gage data is scarce, making analysis of hydrological conditions difficult without the use of remote sensing technology. Much of the study area is dominated by deserts and sparsely vegetated steppes (Klein et al., 2012; Yang et al., 2014). Forests exist in the mountainous regions of Tajikistan and Kyrgyzstan and in the northern parts of Kazakhstan, where more steady precipitation falls throughout the year, as well as in areas closer to the seas and lakes. Little land is cultivated

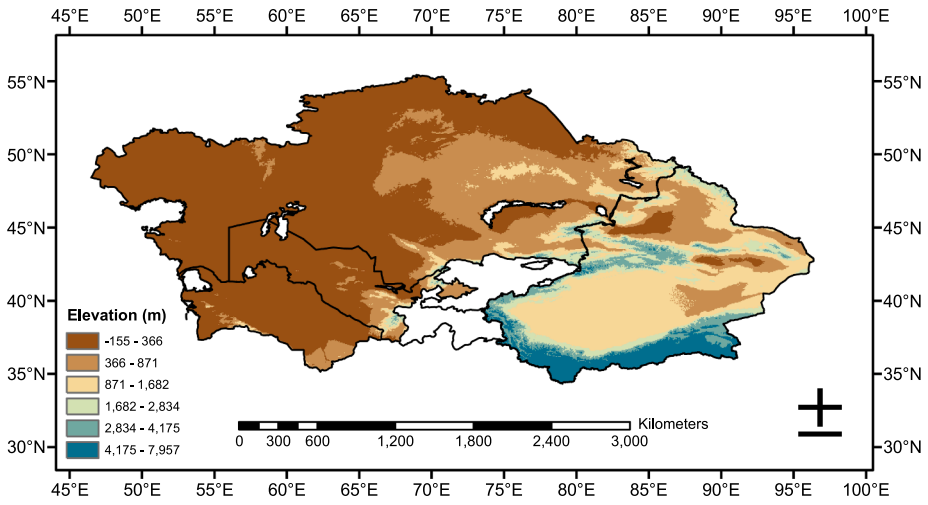

Fig. 1. Map of the study area (Central Asia), derived from GMTED2010 (Danielson and Gesch, 2011).

outside of these regions. Irrigated cropland is sparse, mostly near the various water bodies and mountains, which act as freshwater reservoirs during the dry months of the year.

2.2. *The temporal shift drought analysis framework*

The proposed framework in this paper is an approach to finding propagation time with sub-monthly timescales from meteorological drought to hydrological drought (Fig. 2). This approach uses the run theory to describe the propagation through different types of drought in space and time. Its usefulness is demonstrated in this study using three different hydrological variables representing different parts of the water balance equation (runoff, evapotranspiration, and soil moisture).

The method is as follows:

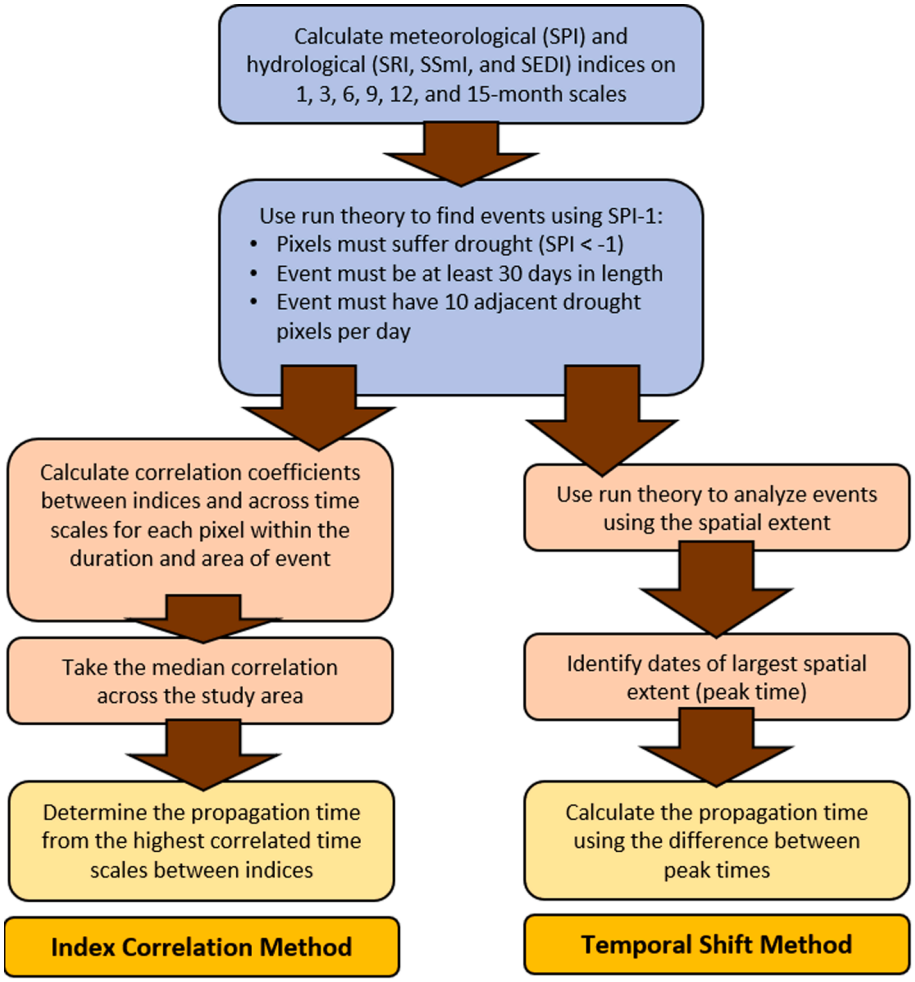

Fig. 2. Methods of calculating propagation time as proposed in this paper.

1. This method is concerned with finding the spatial propagation time—the difference in time between maximum spatial extent in different drought variables—thus, a daily, fine-scale, remote sensing product for each variable is required. This study uses a spatial resolution of 0.25° by 0.25°, though coarser spatial resolutions can be applied.
2. A univariate standardized index is then calculated for each 0.25° by 0.25° pixel and each variable over the record, creating several (one for each variable) time series of drought intensity for each pixel. Observing the most rapid changes, as this study aimed to do, required the use of one-month time scales for all indices.
3. These times series are used to define meteorological drought events; however, there is no universal definition of drought events (Lloyd-Hughes, 2013; Mishra and Singh, 2010; Van Loon, 2015; Zargar et al., 2011). For this study, we use a run theory filter, but different drought definition methods can be substituted if it is possible to identify every pixel undergoing drought conditions at any time step.
4. For each event selected for analysis, the run theory with intensity (standardized index < -1), area (number of adjacent pixels), and duration thresholds is used to reconstruct the spatial expansion of the event.
5. The temporal shifts were then calculated between the peak times, or the time at which the most pixels experience drought, between each hydrologic index and the SPI:

$$t_{shift} = t_{hydro,max} - t_{meteo,max} \quad (1)$$

This temporal shift reflects the response time (propagation time) of maximum hydrological drought area to maximum meteorological drought area. If the peak in the hydrologic index occurs before the SPI (i.e. the shift is negative), it is considered a lead time, whereas if it occurs in the hydrological index first, (i.e. the shift is positive), it is considered a lag time. The definition of characteristics to determine temporal shift can affect the outcome: choosing only the absolute maximum SPI peak time may not be as descriptive as choosing the individual peaks. However, choosing the individual peaks is also problematic because it would then be difficult to ascribe hydrologic peaks to a particular SPI peak, since the number of peaks is often unequal. We therefore calculate temporal shift based on the absolute maximums in the observation window, as they are the most easily identifiable characteristics.

2.2.1. Selected drought indices

Standardized indices use a fitted probability distribution to calculate the number of standard deviations a value is from the average (McKee et al., 1993), a technique that is applicable across different variables and produces meaningful, easily interpreted results. This makes standardized indices reasonable choices for cross-variable comparisons (Farahmand and AghaKouchak, 2015; Hao and AghaKouchak, 2013). Moreover, many studies suggest using a variety of hydrological indicators (Hao and Singh, 2015; Li et al., 2017; Rajsekhar et al., 2015), such as pairings of streamflow and soil moisture, to represent different aspects of the hydrologic cycle. To this end, this study utilizes a total of four standardized and univariate indices (SPI as a meteorological index; and hydrological indices SRI, SEDI, and SSmI, hereafter referred to collectively as SI) to evaluate the propagation of drought in different stages of the water cycle. These indices were calculated using the following remote sensing data sets from the period February 1, 2003 to December 31, 2018 on a daily time step at a resolution of 0.25 by 0.25° (Table 1):

Table 1
Observed variables used in this study and their corresponding drought indices and remote sensing products.

Variable	Product Name	Calculated Index
Precipitation	PERSIANN-CDR	SPI
Total Surface Runoff	GLDAS CLSM v2.2	SRI
AET & PET	GLEAM v3	SEDI
Root Zone Soil Moisture	GLEAM v3	SSmI

- *The Standardized Precipitation Index (SPI)* (McKee et al., 1993) measures the anomaly in precipitation and has been recommended by the World Meteorological Organization as a primary index to characterize such drought (Hayes et al., 2011). It was calculated using PERSIANN-CDR precipitation data (Braithwaite et al., 2015; Nguyen et al., 2019), which is based on satellite observations.
- *The Standardized Runoff Index (SRI)* (Shukla and Wood, 2008) measures the anomaly in generated runoff, which includes both surface runoff and baseflow and is not routed through a river network. Runoff is therefore inclusive of processes that moderate the hydrologic response, such as snow accumulation and melt, and is less sensitive than the SPI in shorter timescales. Longer time scales (e.g. 12 months), despite their higher correlations with longer-scale SPI, are not recommended as they risk integrating values that are beyond the effects of normal hydrologic responses (Shukla and Wood, 2008). The SRI was calculated using the total surface runoff (surface Qs and subsurface runoff Qsb, excluding snowmelt Qsm) from the GLDAS v2.2 Catchment Land Surface Model (Li et al., 2018; Li et al., 2019), which is simulated based on meteorological forcing with data assimilation from the Gravity Recovery and Climate Experiment (GRACE).
- *The Standardized Evapotranspiration Deficit Index (SEDI)* (Vicente-Serrano et al., 2018) measures the evaporative deficit (ED) anomaly, where ED is the difference between the potential evapotranspiration (PET) and the actual evapotranspiration (AET). This definition quantifies the drought stress primarily as lack of water consumed by plants (among other factors) and has low sensitivity to the methodology used to calculate AET. SEDI is characterized "as a short-timescale drought index… [with] sensitivity to high-frequency climate variations", with intended applications in crop and vegetative drought assessment. (Vicente-Serrano et al., 2018) This was calculated using Global Land Evaporation Amsterdam Model (GLEAM) v3.3a products—specifically, the actual evapotranspiration (E) and potential evapotranspiration (Ep) (Martens et al., 2017; Miralles et al., 2011). GLEAM 3.3a is based on both satellite and reanalysis datasets.
- *The Standardized Soil Moisture Index (SSmI)* (AghaKouchak, 2014) measures the deficit anomaly in soil moisture. Accumulated soil moisture deficit is shown to be more persistent than precipitation deficit, has a high autocorrelation factor (indicating strong reliance on previous values), and is less sensitive to rapid developments, resulting in delayed responses to precipitation (AghaKouchak, 2014; Hao and AghaKouchak, 2013; Nicolai-Shaw et al., 2017; 2016) and potentially more persistent drought. This was calculated using GLEAM v3.3a root zone soil moisture data (Martens et al., 2017; Miralles et al., 2011).

Because the goal of the study is to investigate the propagation time of drought as it expands in space, data is required on sub-monthly time scales with a spatial resolution that does not sacrifice detail. Future studies may substitute similar datasets of finer or coarser spatial resolution based on availability; however, records at a daily time step are highly recommended for the successful application of the method proposed in this paper. While many standardized indices require 30 years of data to reliably fit a probability distribution, certain empirical plotting positions—such as the one used in this study—have demonstrated acceptable quality with a sample size of less than 20 (Gringorten, 1963). These can be considered suitable substitutions until enough data is available.

2.2.1.1. Calculation of drought Indices: The standardized drought analysis Toolbox.

The variety of viable distribution curves for standardized

indices represents a challenge for computationally efficient calculations that are justifiable across parameters (Bayissa et al., 2018; Farahmand and AghaKouchak, 2015; Hao and AghaKouchak, 2013; Stagge et al., 2015). The method proposed in the Standardized Drought Analysis Toolbox (SDAT) eliminates these drawbacks by calculating standardized indices based on the empirical probability, which produces similarly valid results in SPI calculation compared to values calculated using the currently-accepted probability distributions (Farahmand and AghaKouchak, 2015). The SDAT uses the empirical Gringorten plotting position to find the probability of occurrence of an observation:

$$p(x_i) = \frac{i - 0.44}{n + 0.12} \tag{2}$$

i is the rank of the observation when ordered from smallest to largest and n is the number of observations (Gringorten, 1963). The resulting probability is used instead of fitted probability distribution functions to calculate the standardized index via the normal inverse:

$$SI = \phi^{-1}(p) \tag{3}$$

More details on the SDAT method can be found in Farahmand and

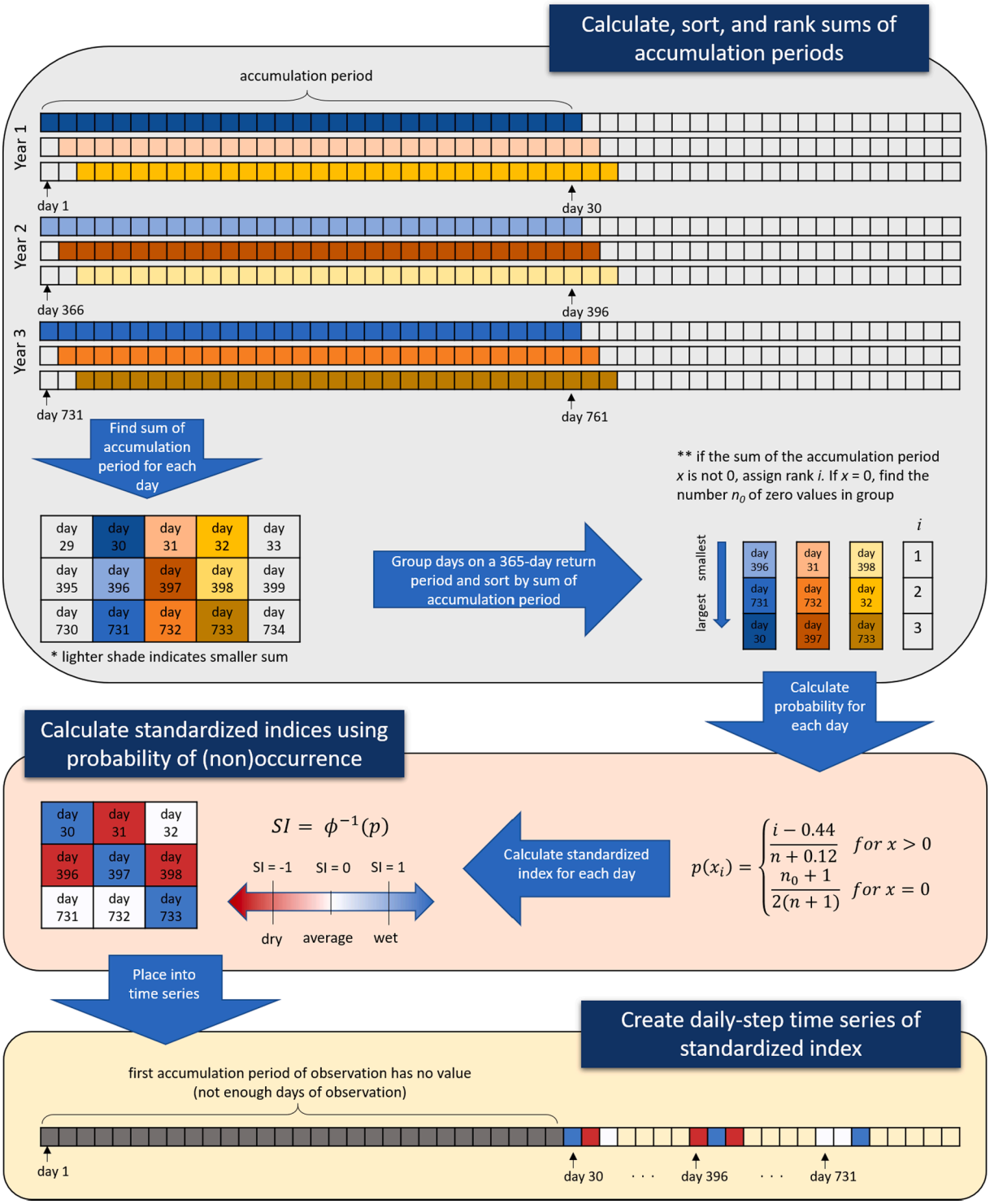

Fig. 3. Process schematic of standardized index time series calculation using the modified Standardized Drought Analysis Toolbox.

AghaKouchak (2015).

In arid and semiarid regions like Central Asia where little to no rainfall or runoff is expected most of the year, it is particularly important to consider the effects of time steps where the accumulated precipitation or runoff is zero. As it increases in frequency, the zero-data condition becomes increasingly problematic: because it is impossible for a drier precipitation or runoff value than zero to occur, using the probability of its occurrence—whether via empirical or fitted distributions—results in an increasingly higher SI. This would falsely imply that the zero-rainfall condition is "wetter" than usual. To compensate for this error, Stagge et al. (2015) demonstrated that using a piecewise function with the Weibull non-exceedance probability to calculate the center of probability mass of multiple zeros results in more statistically meaningful SI values.

In this study, we modify the SDAT source to accommodate zero-data occurrences, as in Stagge et al. (2015), to calculate each of the standardized indices in Table 1. The inclusion of the Weibull non-exceedance probability, which uses the number of zero-data occurrences, n_0, to calculate the probability "center of mass", results in a piecewise function to calculate the probability:

$$p(x_i) = \begin{cases} \dfrac{i - 0.44}{n + 0.12} \; for \; x > 0 \\ \dfrac{n_0 + 1}{2(n+1)} \; for \; x = 0 \end{cases} \quad (4)$$

We also modify the SDAT to accommodate daily-scale remote sensing data (Fig. 3). While commonly calculated for 12 months in a year, the flexibility of the standardized indicator algorithm makes it possible to calculate these indices for every day of the year. Values for each day in the accumulation period—the time scale leading up to and including the current day—are added. Months are assumed to have 30 days each; an accumulation period for a three-month period, for example, would be the previous 90 days. With these adjustments to the source code, the total sum of the observed variable for the accumulation period is calculated, then compared with the same day on a 365-day return period using the combined Weibull non-exceedance probability and empirical Gringorten plotting position.

The recommended dataset length for most standardized indices is 30 years at a monthly time step, which should be sufficient to gather enough data to avoid misleading probabilities (McKee et al., 1993; Stagge et al., 2015). The use of the Gringorten empirical plotting position similarly recommends sample sizes of 20 or more (in this context, 20 years of data or more) but can still produce adequate results with fewer data points (Gringorten, 1963). This length and quality of record is currently not possible for all remote sensing products, especially on such fine temporal and spatial resolutions; thus, the calculation uncertainty of the probability and resulting standardized index is noted, but currently unavoidable. However, further development of daily-scale methods and analyses despite these challenges will be necessary to investigate seasonal to sub-seasonal flash drought events (Pendergrass et al., 2020).

2.3. Definition of drought events using the run theory

The run theory was first adapted for use in analysis of drought by Yevjevich (1967) to describe large continental hydrologic droughts. This theory defines a drought event as a period or "run" over which the observation of a variable meets a minimum threshold in an area. Depending on what parameters or approaches are selected, additional factors should be considered. This application allows identification of descriptors such as starting time, duration, and peak time, making possible the calculation of different temporal shifts. Despite frequent usage of the run theory for drought composite analyses (Keyantash and John, 2002; Tallaksen et al., 2009; Van Loon et al., 2012; Zhu et al., 2016), it has very seldom, if ever, been used to calculate drought propagation time on a sub-monthly scale.

To determine and define drought events for analysis, we employ a run theory algorithm which exists separately from the proposed framework and uses a clustering algorithm similar to the one defined by Andreadis et al. (2005). A "run" begins when a cluster appears that breaches a spatial and intensity threshold. However, unlike in Andreadis et al. (2005), cluster cells must share sides; cells sharing corners are not considered. Each day may have multiple clusters throughout the study area, and these clusters may have oblong shapes. If 30 consecutive days have drought clusters, that grouping of days is considered a drought candidate. Then, from each drought candidate, an event is reconstructed by selecting the largest cluster and pulling from each day in the candidate all other clusters that contain at least one pixel from that largest cluster.

Spatial thresholds vary between drought identification studies, particularly in response to the size of the study area and the study objectives. In their study over the conterminous U.S., Andreadis et al. (2005) used a minimum cluster size of 10 pixels (on a 0.5° degree resolution, roughly 30,000 km^2). Meanwhile, a study over China by Wang et al. (2011) uses an area of 150,000 km^2 to identify previous events. When searching on a global context, Sheffield et al. (2009) found that a minimum area of 500,000 km^2 minimized improper drought event persistence across continents; Lloyd-Hughes (2012) uses this same area threshold in their study over Europe. However, these studies searched for large drought events—in this study, we are interested in observing a drought event from its beginning to end, regardless of its size. Future studies may use size thresholds that are more suited to their desired objectives. Thus, we follow the example of Andreadis et al. (2005): each cluster must consist of an area larger than 10 pixels (spatial threshold) with SPI $<= -1$ (intensity threshold).

More sophisticated algorithms and theories exist for defining and identifying drought events and can be used with this proposed propagation time calculation, as long as it is possible to find all pixels experiencing drought at each time step. Guo et al. (2018b) developed a three-dimensional drought clustering system to define other events in Central Asia, while Li et al. (2020) proposed a method unique to flash droughts that could be modified for normal droughts. A study by Bayissa et al. (2018) showed that, of six drought indices, no single index could capture every onset in a basin in Ethiopia, indicating that more variables could be included in future improvements to drought identification algorithms. However, furthering the discussion of defining drought is beyond the scope of our study.

2.4. The correlation method

The classical approach to finding the propagation time from one index to another, which is to find the highest-correlated time scales, was applied to individual drought events. Standardized indices at various time scales were considered for this index correlation analysis using the Pearson correlation coefficient. All indices and time scales were cropped to the maximum area extent and duration of each SPI event (the long, medium, short, and very short events). This ensured that we were only observing pixels that were involved in the drought event and compared exclusively during the duration of the event. The Pearson correlation coefficient was then calculated for each pixel in the event and filtered for only significant ($p <= 0.05$) correlations, and the median was calculated across the event's extent as the final value. The median was chosen because of the sensitivity of the average to the existence of high correlations and anticorrelations, which were present for individual pixels in the event. This method is based on two assumptions: first, that the meteorological drought is the driver of hydrological drought, and that the propagation time is the hydrological index time scale that is highest correlated.

In the literature, this analysis is typically performed with the hydrological index fixed at one month (SI-1) with SPI calculated at different time scales. However, correlations with SI-1 can be

Table 2
List of discovered drought events with corresponding maximum area (in pixels), duration, and length categories. Pixels are 0.25 × 0.25°each, or roughly 770 km^2.

	Start	End	Maximum Size (# of pixels)	Length (days)	Classification	Agreeance with GDO
1	5-Mar-03	16-Aug-04	3680	530	long	Yes
2	18-Aug-04	24-Dec-04	1457	128	short	Yes
3	5-Jan-05	28-Jan-06	4724	388	long	Yes
4	28-Feb-06	30-Oct-06	5019	244	medium	Yes
5	6-Nov-06	3-Oct-08	6445	697	long	Yes
6	7-Oct-08	17-Dec-09	7222	436	long	Yes
7	19-Dec-09	18-Feb-10	1120	61	short	
8	28-Mar-10	6-Jan-13	6478	1015	long	Yes
9	18-Feb-13	20-Aug-13	1536	183	medium	
10	29-Aug-13	17-Dec-13	4749	110	short	Yes
11	2-Jan-14	15-Mar-14	1161	72	short	
12	24-Mar-14	21-Oct-14	2742	211	medium	Yes
13	9-Feb-15	18-Apr-15	2376	68	short	
14	24-Apr-15	3-Nov-15	3142	193	medium	Yes
15	2-Feb-16	1-Apr-16	4946	59	very short	
16	12-May-16	12-Jun-16	399	31	very short	
17	16-Jun-16	17-Jul-16	246	31	very short	
18	17-Aug-16	9-Nov-16	940	84	short	
19	14-Jan-17	8-May-17	2233	114	short	
20	15-May-17	6-Apr-18	2010	326	medium	
21	25-Apr-18	26-Nov-18	2124	215	medium	

inconclusive; therefore, we broadened the analysis to include correlations with SI at different time scales. To observe the effects of meteorological droughts on other types of drought, it is necessary that the second index has a time scale that is less than or equal to the SPI time scale (SI-n <= SPI-m). This is because of the way that the standardized indices are calculated: a longer time scale means a longer period before the current day is considered. That means that, for an analysis showing the propagation from meteorological to hydrological drought, we should only include correlations for which the meteorological index includes more time than the hydrological index.

Correlation analysis is commonly applied in research of all disciplines, making its limitations well-known (Schober et al., 2018; Taylor, 1990). Though there are commonly accepted ranges for goodness of fit criteria (including correlation) in the field of hydrological modeling, they are typically applied for calibration and validation evaluation. From this perspective, then, a selection of two well-correlated time scales could mean a "calibration" of one index to another; however, such a perspective must also consider the risks of blindly choosing the highest correlated indices (overfitting), especially when considering the existence of several comparably high correlation coefficients.

There are additional issues specific to application of correlation analysis in propagation time. Because correlation between time series is independent of order (it does not matter if the SPI peaked before another index or vice versa), an assumption must be made for which drought event comes first. We assumed, as many in the literature did, that precipitation drought drives other forms of drought (Barker et al., 2016; Huang et al., 2017; Van Loon, 2015; Xu et al., 2019). Hence, propagation times calculated using the correlation method are assumed to be from meteorological drought to hydrological drought.

3. Results & discussion

3.1. Drought identification

3.1.1. Drought events

While a detailed discussion of the merits of a particular identification approach are beyond the scope of this paper, it is still necessary to ensure that the results generally agree with historical drought conditions. The run theory definition in this paper produced 21 unique drought events of varying lengths and maximum area extents (Table 2), of which seven loosely agree in time and space with events found in the European Commission's development of a Global Drought Observatory (GDO) (Spinoni et al., 2019). Identified droughts in this study are not expected to be in strong agreement with the literature due to different drought definition criteria: the GDO uses both the SPI and the SPEI at the 3-, 6-, and 12-month levels between 1951 and 2016 and removed any drought events that did not last for at least two months, that occurred too close to the end of a previous drought event, and that did not grow sufficiently large (Spinoni et al., 2019). In contrast, our droughts are simply defined with a small spatial threshold, a minimum length of 30 days, and on a 1-month time scale with no further filtering criterion. Of particular importance was the identification of the 2008–2010 drought in Central Asia, which was noted as one of the world's most extreme by several studies (Guo et al., 2018a; Spinoni et al., 2019). That this drought identification algorithm was able to identify key events allows for further analysis of its results.

Most identified drought events were between 30 and 180 days. Drought events were then classified as very short, short, medium, or long events based on their duration (Table 3). The largest drought of each length category was selected as a representative for further visual analysis of spatial and temporal propagation. The largest events would have the most easily identifiable characteristics using this method since it is based on affected area—larger events will have more exaggerated characteristics. However, this method can be applied for smaller events as well. The maximum spatial extents of each representative event can be seen in Fig. 4.

Because this method aims to look at the spatial propagation time, drought selection criteria must be able to consider the size of the drought event and be flexible enough to accommodate changing sizes. Plots of drought intensity averaged over the event's area (Fig. 5) can demonstrate the relationships between the magnitude of different indices. However, this lacks the consideration of spatial variability, as an average or even sum of values eventually assigns a single value to the study area. Intensity is therefore only applied in this study as a binary filter for determining if a cell is experiencing drought. However, because it is one of the main dimensions of drought, future studies in spatial propagation may consider adding an additional factor for intensity.

3.2. Propagation time

3.2.1. Correlation

A heat map of statistically significant correlations between all relevant time scales for the representative events can be seen in Fig. 6. If the SPI time scale that correlates the strongest to SI-1 is the propagation

Table 3
Ranges of duration for proposed drought length classifications.

Length classification	Duration (days)	Number of events
Long	366+	5
Medium	181–365	6
Short	61–180	7
Very short	30–60	3

time (as many studies have assumed), then the propagation times for SRI would be 3 months for the very short event, 1 month for the short event, 1 month for the medium event, and 1 month for the long event; for SSmI, it would be 6 months, 3 months, 3 months, and 6 months respectively; and for SEDI, it would be 6 months, 1 month, 3 months, and 3 months. The strength (or lack thereof) of the SEDI correlations indicate that this analysis could be insufficient, though the trend of higher correlations at longer timescales is consistent with the literature (Kim et al., 2019). It is therefore difficult to decisively say that a single pair of highly correlated time scales is a propagation time; rather, a range of time scales could be considered. Furthermore, as medians, these values ignore the spatial variability of the catchment. Individual cells may have had extremely high correlation or anticorrelation that was lost when calculating the median value. Future investigation could discern why certain pixels had high correlation while others did not.

Overall, the highest correlated time scales for the very short event are SPI-3 and SRI-3, SPI-6 and SSmI-3, and SPI-6 and SEDI-1; for the short event, SPI-1 and SRI-1, SPI-3 and SSmI-1, and SPI-9 and SEDI-9; for the medium event, SPI-9 and SRI-9, SPI-12 and SSmI-9, and SPI-15 and SEDI-15; and for the long event, SPI-12 and SRI-12, SPI-6 and SSmI-3, and SPI-15 and SEDI-12. Despite the inclusion of more data points, there is still no clear highest correlation in some of the drought events—rather, there are several high median correlation coefficients which could be similarly effective. Analyses of these pairs should consider, however, that longer time scales generally result in higher correlation as discussed in Shukla and Wood (2008).

Additional time scale considerations include relevancy to the index. The SRI and SEDI are shorter-time-scale indices by virtue of their observed variable. While evaporative deficits calculated over longer time scales can be indicative of agricultural productivity (Kim et al., 2019), the extreme volatility of evaporative conditions can make it very

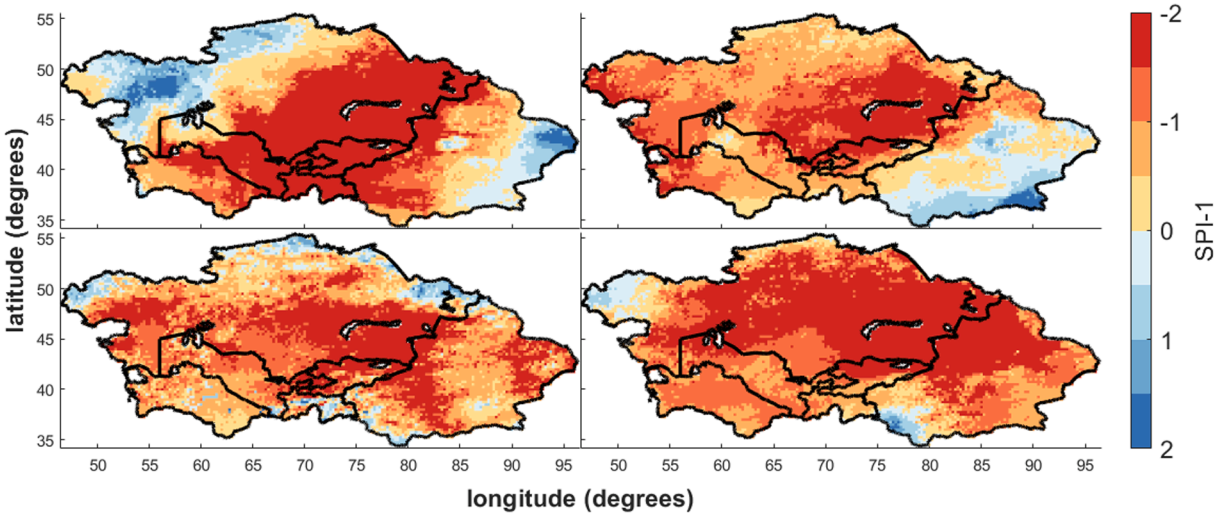

Fig. 4. Plots of maximum spatial extents and intensity of each of the selected drought events (top left: very short, top right: short, bottom left: medium, bottom right: long).

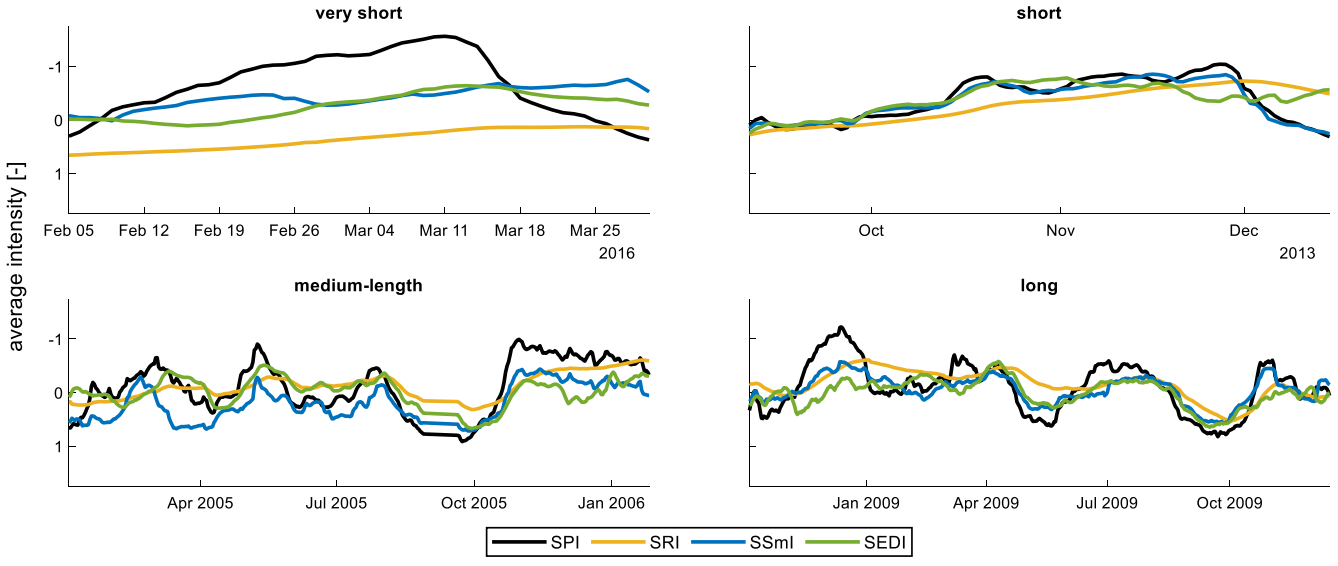

Fig. 5. Plots of intensity for the four representative drought events averaged over the event's maximum spatial extent.

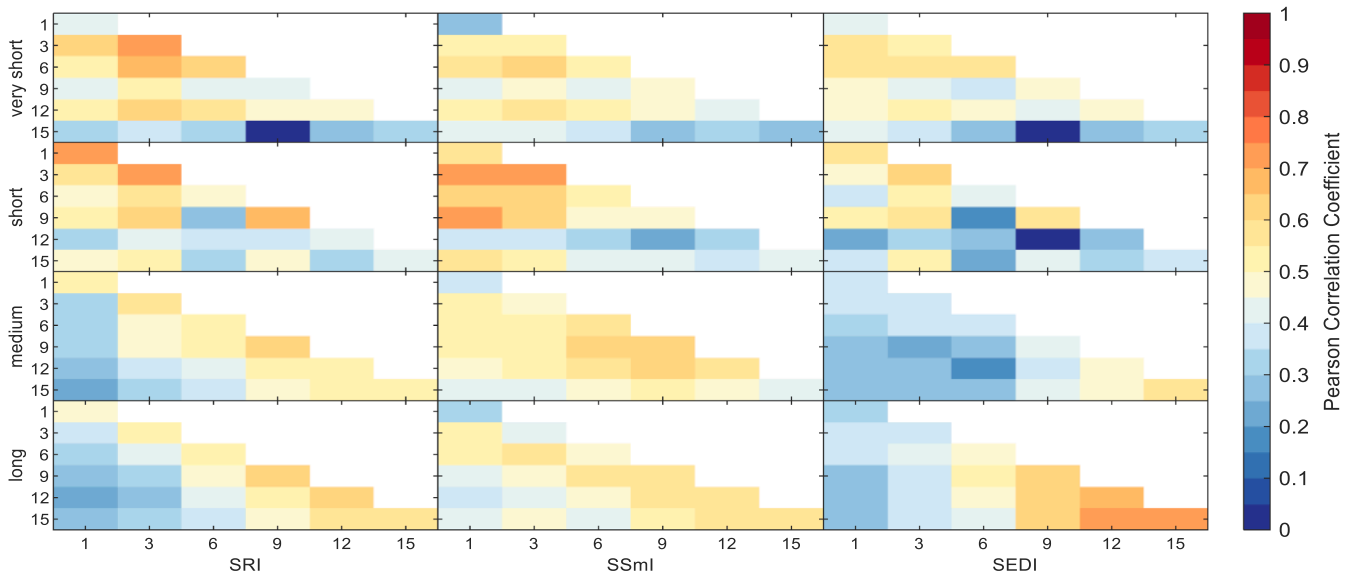

Fig. 6. Heat map of median correlations for representative events between SPI (y-axis) and hydrological indices (x-axis) for different time scales.

useful at short time scales (Vicente-Serrano et al., 2018), especially in cases of rapidly developing flash drought (Li et al., 2020). Generated runoff is a valuable index because generated runoff includes hydrological attenuating processes, but time scales that are too long run the risk of including processes that are no longer relevant for current runoff shortages; however, this also depends on climate and precipitation regimes, as precipitation as snowmelt could affect runoff generation later in the year (Shukla and Wood, 2008). Root zone soil moisture observations, however, show high autocorrelation, higher persistence, and are less volatile (AghaKouchak, 2014; Narasimhan and Srinivasan, 2005; Nicolai-Shaw et al., 2017; 2016); here, it could be important to consider longer time scales.

These considerations are not always reflected in the results: in general, as the length of the event increases, the highest correlated time scales also increase. This is rather expected for soil moisture drought, as a persistence-based drought index would presumably correlate higher at longer accumulation periods, regardless of event length. The supposedly short-term nature of the SEDI makes its highest correlated indices in all but the very short event surprising. This could be the byproduct of increasing scale, as Shukla and Wood (2008) noted, since increasing the scale of the index smooths the resulting time series curves: as the accumulation period increases, the curves converge. This could also be a reason why the SRI's highest correlated time scales jump from subseasonal to almost yearly scales in longer events.

3.2.2. *Temporal shift*

Final plots of each run theory analysis for the representative events can be seen in Fig. 7, with the corresponding temporal shifts in Table 4. The SPI area (black) is plotted for only the duration of the event, while the hydrological time series include additional time windows for visual context only. The very short drought event demonstrates a simple run of drought area, with only one peak. As expected, the SRI and SEDI in this event seem to respond quickly to the increase in SPI area, while the SSmI lags in both spatial extent and time. The short event shows more complexity as it expands and contracts during the duration of the event. While the SRI again shows quick responses to changes in SPI and the SSmI a more muted response, the SEDI demonstrates surprising behavior by peaking while the SPI event contracts. The difference is also not a lag but a lead time from SRI and SEDI peaks to an SPI peak. Such an expansion in area in a hydrologic index before a meteorological index signals that hydrological drought in various forms may not always be driven by rainfall deficit—hydrological drought may, as with many hydrologic phenomena, be influenced by additional variables, a finding corroborated by studies in flash drought (Ford and Labosier, 2017; Mo and Lettenmaier, 2015; Otkin et al., 2018). These could be, for example, a heat wave flash drought causing an increase in evapotranspiration (Mo and Lettenmaier, 2015) and reducing generated runoff despite a precipitation event (indicated by the decrease in SPI), a likely scenario in this study area. This underscores the importance of a holistic view of drought: no single index can capture all of these changes.

This complex behavior becomes more apparent in the medium-length and long drought events. These events are marked by strong successive signals that contract and almost disappear before expanding again, indicating that long drought events can be a series of smaller drought events. Such signals could be broken into smaller drought events using, for example, a higher drought area threshold or a different clustering algorithm.

The results of temporal shift analyses for almost all identified events, sorted by length category, are summarized in Fig. 8. For clarity, separate axes are used for each length category. Because standardized indices require a period of observation before the date of calculation, this acts as a "warm up period" for calculation (Fig. 3). For this "warm up period", the drought conditions are unknown. Thus, it is unclear when the first observed drought event, which "begins" at the beginning of the record, actually begins and is therefore excluded from this analysis because of the potential skew on the data.

In general, the range of temporal shifts increase in proportion to the length category. This general increase is expected, as a longer event length means potentially more drought subpeaks and therefore more chances for a larger area to occur. Closer inspection of the results by observed variable can assist the identification of factors influencing drought propagation in space and time.

The SSmI almost exclusively exhibits lag times; the single exception is a short event that occurs almost immediately after a long event (event 2 in Table 2). Soil moisture—and the SSmI—exhibits high autocorrelation (AghaKouchak, 2014; Narasimhan and Srinivasan, 2005); in other words, its current value is strongly dependent on historical values and changes slowly in comparison to the other hydrological variables. In this study area, long lag times are likely due to the lack of dense vegetation cover accelerating desertification and increasing evaporation from the bare soil (Li et al., 2017; Patrick, 2017); however, because root zone soil moisture shows high persistence (AghaKouchak, 2014; Nicolai-Shaw et al., 2016), this could cause long drought development periods and a delayed peak. Recovery of deficits in the root zone will also take longer

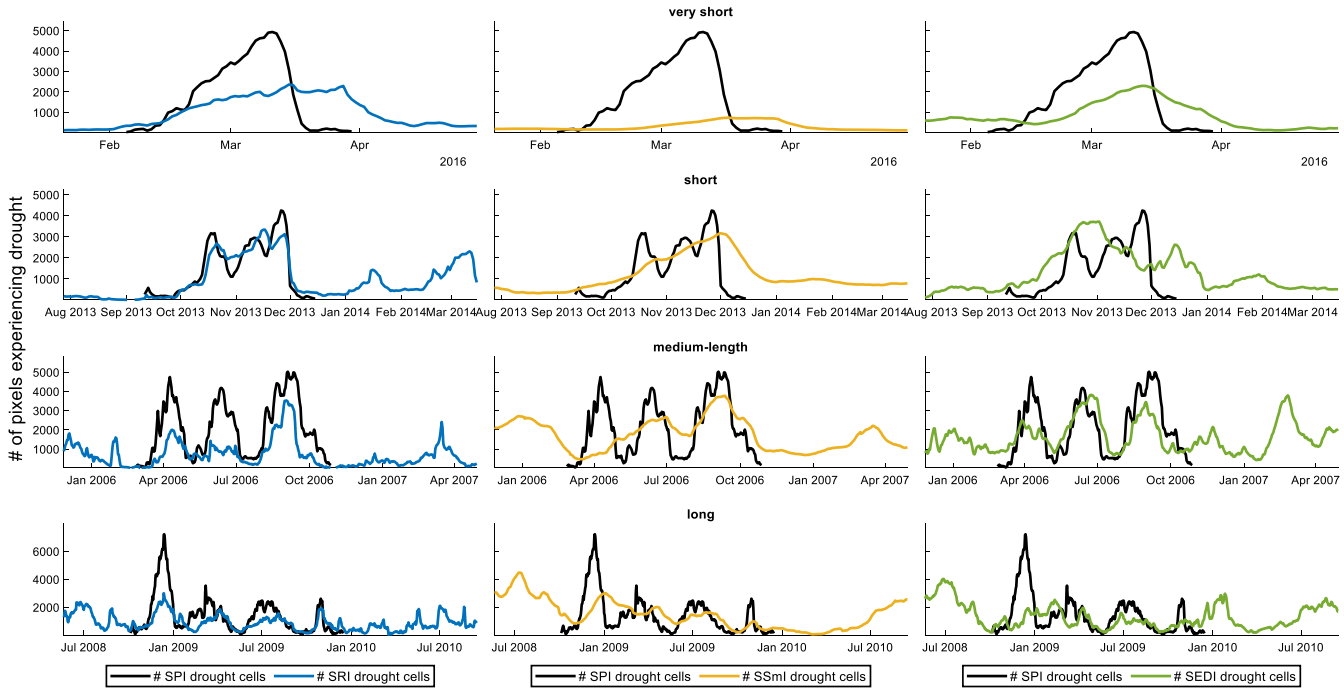

Fig. 7. The development of drought size (expressed as pixels) in time between SPI and different hydrologic indices.

Table 4
Results of the temporal shift method, describing the lag (+) or lead (-) time, in days, for each hydrologic index in each representative event.

Very short			Short			Medium			Long		
SRI	SSmI	SEDI	SRI	SSmI	SEDI	SRI	SSmI	SEDI	SRI	SSmI	SEDI
4	6	2	−9	5	−24	2	12	−68	−1	22	60

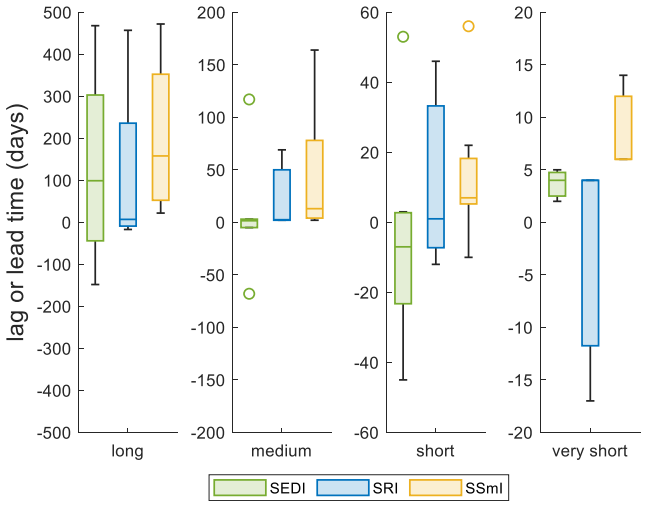

Fig. 8. Results of the temporal shift analysis, lag (+) or lead (-) times (in days), for all events identified, sorted by length category: long (n = 4), medium (n = 6), short (n = 7), very short (n = 3). Note that the axes are different for each category.

than surface soil moisture (Nicolai-Shaw et al., 2017). The resultant persistent nature of SSmI in this study region could therefore mean that the beginning of the event (as defined by the SPI) coincides with the preceding event's recovery and should be viewed critically, while prevention of similar instances can be achieved using additional filters when determining drought.

In comparison, the SRI is less predictable as it can be either a lead or a lag time. When it is a lead time, it is within 20 days of an SPI peak. When it is a lag time, however, its duration is highly variable. That its median remains close to zero is an indication of the strong relationship between runoff and precipitation, though this could change as more events are analyzed. The wide range of values reflects the impact that factors aside from precipitation—such as land cover, soil type, and initial conditions—can have on runoff generation. Increases in surface evaporation through high temperatures or low humidity, for example, could decrease the surface soil moisture. Dry antecedent conditions can decrease runoff from precipitation, requiring more moisture to saturate the top soil layer before becoming runoff (Castillo et al., 2003; Kirchner, 2009). This could create runoff deficits when decreases in SPI would indicate a recovery period, as in the short representative event (Fig. 7). In general, though, the tendency of SRI to have lag rather than lead times indicates that runoff drought propagates largely from precipitation drought.

Like the SRI, the median SEDI propagation time fluctuates; however, the SEDI is even less predictable with a broader range of propagation times. This is likely a reflection of the various factors on which evapotranspiration is dependent. Unlike soil moisture and runoff, evapotranspiration and its deficit are not explicitly dependent on a precipitation input. Typical evapotranspiration estimation models use temperature, humidity, radiation, and even vegetation cover as input: in this context, precipitation as available water provides an upper limit for evapotranspiration but is not one of the main influencing factors. Thus, it can be said that evaporative deficits are influenced by—but not necessarily derived from—precipitation deficits. These findings are consistent with recent literature on flash drought (Ford and Labosier, 2017; Hobbins et al., 2016; Mo and Lettenmaier, 2015; Otkin et al., 2018), where precipitation is not identified as a main driver. Instead, a combination of high temperatures, low humidity, and increased solar radiation are likely candidates for increases in evaporative deficits

independent of precipitation (Ford and Labosier, 2017; Mo and Lettenmaier, 2015).

In contrast to the range, trends in the precise propagation time as duration increases are not as straightforward. A scatter plot of the temporal shift (y-axis) and the event duration (x-axis) is given in Fig. 9. In addition to the event excluded in the previous analysis, two other events were excluded: because they were the only two events that lasted more than 450 days (697 and 1015 days in length), they can reasonably be considered outliers. A linear regression analysis of the 18 remaining points indicates there is a slight trend in propagation time as drought duration increases; however, the low correlation indicates the length and temporal shift are largely unrelated. It is important to note that the sample size is low—thus, further experimentation with this method is needed to reach a decisive conclusion on trends between drought length and propagation time.

3.2.3. *Differences between the temporal shift and correlation methods*

The estimates from the temporal shift and correlation methods differ greatly, indicating that they describe different processes. The time scale correlation is the median of the correlations in all cells the drought-affected area, which effectively ignores the spatial variability of the study area. In a continental-scale study area like Central Asia, this assumption of spatial uniformity is not valid. Even after narrowing down the region to specific drought areas, such analysis demands a single correlation per drought, which can extend over more than half the region (Fig. 4); thus, the correlation method is incapable of producing a spatial propagation time. However, because it is a comparison between two intensity time series, it may describe the propagation of drought intensity.

Aside from the validity of this spatial generalization, the meaning of the highest-correlated time scales is unintuitive. The extraction of the propagation time from this method is still unclear—moreover, it would be an estimate on a monthly scale (Fig. 6). In contrast, the temporal shift analysis offers a more straightforward interpretation of propagation that includes a higher precision and consideration of spatial variability. Such precision is valuable when trying to find trends in propagation time, which are necessary to develop a better understanding of propagation mechanics, and for rapidly developing flash drought events where a monthly resolution would result in a significant lack of detail (Otkin et al., 2018; Pendergrass et al., 2020). Moreover, runoff and evapotranspiration drought often preceded meteorological drought (Fig. 8), indicating that the assumption of meteorological drought propagating into hydrological drought is not always valid. Thus, the temporal shift method provides a clearer and finer-resolution estimate of propagation time that avoids the problematic assumptions of the correlation method.

3.2.4. *Limitations of the temporal shift*

A major limitation is the definition and selection of drought events, though this is again a limitation that is not unique to this study. In this study, we do not consider the lingering effects of drought events that occur shortly after another, which could potentially accelerate certain processes or affect the temporal shift. An example of this is events 1 & 2 in Table 2, which resulted in the sole negative temporal shift in SSmI. Other studies have used complex algorithms to refine selection of drought events to exclude such events—with this filtering, an application of the drought propagation time methods in this paper may produce clearer results. As noted in Yevjevich (1967), proper selection of a minimum threshold will also greatly affect results. In other words, a proper selection of drought events through filtering strategies and time windows for study can minimize the lingering effects of one drought event onto another.

The temporal shift approach is heavily dependent on the observed characteristics. Fig. 7 demonstrates that longer drought events are made of smaller sub-droughts—this complicates the issue of determining which characteristics of the run to observe. Choosing the largest peaks, as in this study, is a straightforward and universally applicable strategy; however, the rapid responses of SEDI and SRI to SPI indicate that it could be possible to pair sub-peaks in those indices. This requires further research to improve justification of which peaks to pair: our analysis demonstrates that hydrological expansion before meteorological expansion is possible, so simply choosing the next subsequent sub-peak may not be logical.

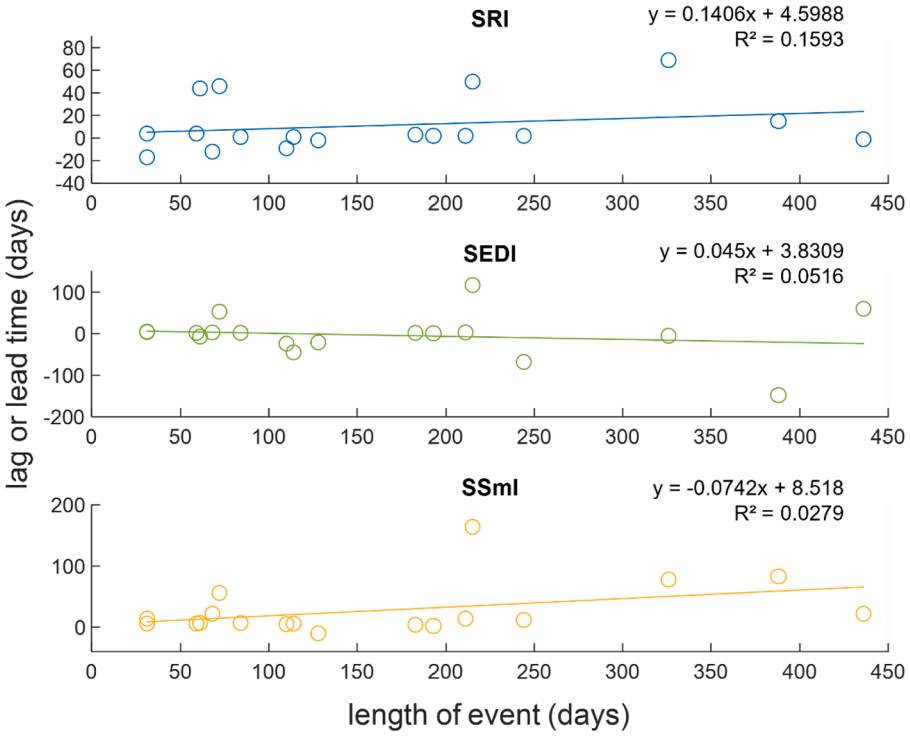

Fig. 9. Scatter plot and linear regression of temporal shift in days (y-axis) and event duration (x-axis) for the region of highest density (n = 18).

4. Conclusion

The framework proposed in this paper is among the first to attempt to determine the spatial propagation time with higher (sub-monthly) precision for sub-continental regions. This method leverages recently developed high-resolution remote sensing data to apply the run theory to determine the propagation time for individual drought events. The framework was applied to propagation in runoff, evapotranspiration, and soil moisture droughts to provide hydrological context for different propagation times. In some events relating to runoff and evapotranspiration deficits, hydrological drought persists and even increases despite precipitation events, indicating that precipitation alone does not always drive hydrological drought events. The varying lag or lead times for evapotranspiration and runoff drought reflect that many other factors impact these processes aside from precipitation—for example, land cover, soil type, temperature, and humidity—and that these factors give important contextual information about how drought develops. In contrast, soil moisture drought quite consistently shows a delayed response to meteorological conditions, a reflection of the prominent role that precipitation plays in root zone soil moisture levels and the strong dependence on soil moisture from the previous day.

The temporal shift can be understood as the interval during which the affected area of one hydrological variable's deficit responds to another, or the spatial propagation time; in contrast, the traditional correlation analysis may describe propagation of other drought elements such as intensity. However, the assumption of spatial uniformity inherent from the correlation analysis may not be valid for sub-continental and continental scale regions and can result in poorly correlated results. Moreover, the results of the temporal shift analyses demonstrate that the correlation method's assumption of precipitation-driven drought may not always hold. In this context, the temporal shift method presents key advantages over the correlation analysis such as consideration of spatial variability, precision, different drivers, and ease of interpretation.

While the framework in this study presents new clarity into drought propagation through different hydrologic variables, it requires resolution of several challenges. The uncertainty in standardized index calculation, for example, should be reduced with longer periods of observation. Further investigation should advise considerations on what characteristics of a run are most descriptive for determining propagation. Advanced drought identification techniques can reduce interference of potentially unrelated events during the analysis; the standardization of such algorithms will prove incredibly useful for application of this method in different studies. However, the novel application of a run theory analysis on univariate standardized drought indices calculated on a daily scale presents new opportunities for the investigation of drought—in particular, fast-developing flash drought events.

CRediT authorship contribution statement

Sarah Quynh-Giang Ho: Formal analysis, Methodology, Visualization, Writing – original draft, Writing – review & editing. **Lu Tian:** Conceptualization, Methodology, Writing – review & editing. **Markus Disse:** Resources, Writing – review & editing. **Ye Tuo:** Conceptualization, Methodology, Supervision, Writing – review & editing.

Declaration of Competing Interest

The authors declare that they have no known competing financial interests or personal relationships that could have appeared to influence the work reported in this paper.

Acknowledgements

The authors would like to thank the editors and anonymous reviewers for their insightful comments. Additional thanks to Dionisio Vendrell Jacinto, M.Sc., for his help with programming the algorithms to identify drought clusters. Lu Tian acknowledges the financial support from the China Scholarship Council. This research did not receive any specific grant from funding agencies in the public, commercial, or not-for-profit sectors.

References

AghaKouchak, A., 2014. A baseline probabilistic drought forecasting framework using standardized soil moisture index: application to the 2012 United States drought. Hydrol. Earth Syst. Sci. 18 (7), 2485–2492. https://doi.org/10.5194/hess-18-2485-2014.

Andreadis, K.M., Clark, E.A., Wood, A.W., Hamlet, A.F., Lettenmaier, D.P., 2005. Twentieth-century drought in the conterminous United States. J. Hydrometeorol. 6 (6), 985–1001.

Barker, L.J., Hannaford, J., Chiverton, A., Svensson, C., 2016. From meteorological to hydrological drought using standardised indicators. Hydrol. Earth Syst. Sci. 20 (6), 2483–2505. https://doi.org/10.5194/hess-20-2483-2016.

Bayissa, Y., et al., 2018. Comparison of the performance of six drought indices in characterizing historical drought for the upper blue nile basin. Ethiopia. Geosciences 8 (3). https://doi.org/10.3390/geosciences8030081.

Beguería, S., Vicente-Serrano, S.M., Reig, F., Latorre, B., 2014. Standardized precipitation evapotranspiration index (SPEI) revisited: parameter fitting, evapotranspiration models, tools, datasets and drought monitoring. Int. J. Climatol. 34 (10), 3001–3023.

Braithwaite, D.K., et al., 2015. PERSIANN-CDR: daily precipitation climate data record from multisatellite observations for hydrological and climate studies. Bull. Am. Meteorol. Soc. 96 (1), 69–83. https://doi.org/10.1175/bams-d-13-00068.1.

Castillo, V., Gomezplaza, A., Martinezmena, M., 2003. The role of antecedent soil water content in the runoff response of semiarid catchments: a simulation approach. J. Hydrol. 284 (1–4), 114–130. https://doi.org/10.1016/s0022-1694(03)00264-6.

Crausbay, S.D., et al., 2017. Defining ecological drought for the twenty-first century. Bull. Am. Meteorol. Soc. 98 (12), 2543–2550. https://doi.org/10.1175/bams-d-16-0292.1.

Danielson, J.J., Gesch, D.B., 2011. Global multi-resolution terrain elevation data 2010 (GMTED2010). US Department of the Interior, US Geological Survey.

Farahmand, A., AghaKouchak, A., 2015. A generalized framework for deriving nonparametric standardized drought indicators. Adv. Water Resour. 76, 140–145. https://doi.org/10.1016/j.advwatres.2014.11.012.

Ford, T.W., Labosier, C.F., 2017. Meteorological conditions associated with the onset of flash drought in the Eastern United States. Agric. For. Meteorol. 247, 414–423. https://doi.org/10.1016/j.agrformet.2017.08.031.

Gevaert, A.I., Veldkamp, T.I.E., Ward, P.J., 2018. The effect of climate type on timescales of drought propagation in an ensemble of global hydrological models. Hydrol. Earth Syst. Sci. 22 (9), 4649–4665. https://doi.org/10.5194/hess-22-4649-2018.

Gringorten, I.I., 1963. A plotting rule for extreme probability paper. J. Geophys. Res. 68 (3), 813–814.

Guo, H., et al., 2018a. Spatial and temporal characteristics of droughts in Central Asia during 1966–2015. Sci. Total Environ. 624, 1523–1538. https://doi.org/10.1016/j.scitotenv.2017.12.120.

Guo, H., et al., 2018b. Space-time characterization of drought events and their impacts on vegetation in Central Asia. J. Hydrol. 564, 1165–1178. https://doi.org/10.1016/j.jhydrol.2018.07.081.

Guo, Y., et al., 2020. Propagation thresholds of meteorological drought for triggering hydrological drought at various levels. Sci Total Environ 712, 136502. https://doi.org/10.1016/j.scitotenv.2020.136502.

Hao, Z., AghaKouchak, A., 2013. Multivariate standardized drought index: a parametric multi-index model. Adv. Water Resour. 57, 12–18. https://doi.org/10.1016/j.advwatres.2013.03.009.

Hao, Z., Singh, V.P., 2015. Drought characterization from a multivariate perspective: a review. J. Hydrol. 527, 668–678. https://doi.org/10.1016/j.jhydrol.2015.05.031.

Hayes, M., Svoboda, M., Wall, N., Widhalm, M., 2011. The lincoln declaration on drought indices: universal meteorological drought index recommended. Bull. Am. Meteorol. Soc. 92 (4), 485–488. https://doi.org/10.1175/2010bams3103.1.

Hobbins, M.T., et al., 2016. The evaporative demand drought index. Part I: linking drought evolution to variations in evaporative demand. J. Hydrometeorol. 17 (6), 1745–1761. https://doi.org/10.1175/jhm-d-15-0121.1.

Huang, S., et al., 2017. The propagation from meteorological to hydrological drought and its potential influence factors. J. Hydrol. 547, 184–195. https://doi.org/10.1016/j.jhydrol.2017.01.041.

Jehanzaib, M., Sattar, M.N., Lee, J.-H., Kim, T.-W., 2019. Investigating effect of climate change on drought propagation from meteorological to hydrological drought using multi-model ensemble projections. Stoch. Env. Res. Risk Assess. 34 (1), 7–21. https://doi.org/10.1007/s00477-019-01760-5.

Keyantash, J.A., Dracup, J.A., 2004. An aggregate drought index: Assessing drought severity based on fluctuations in the hydrologic cycle and surface water storage. Water Resour. Res. 40 (9) https://doi.org/10.1029/2003wr002610.

Keyantash, J.D., John, A., 2002. The quantification of drought: an evaluation of drought indices. Am. Meteorol. Soc.

Kim, D., Lee, W.S., Kim, S.T., Chun, J.A., 2019. Historical drought assessment over the contiguous united states using the generalized complementary principle of

evapotranspiration. Water Resour. Res. 55 (7), 6244–6267. https://doi.org/10.1029/2019wr024991.
Kirchner, J.W., 2009. Catchments as simple dynamical systems: catchment characterization, rainfall-runoff modeling, and doing hydrology backward. Water Resour. Res. 45 (2) https://doi.org/10.1029/2008wr006912.
Klein, I., Gessner, U., Kuenzer, C., 2012. Regional land cover mapping and change detection in Central Asia using MODIS time-series. Appl. Geogr. 35 (1–2), 219–234. https://doi.org/10.1016/j.apgeog.2012.06.016.
Li, B., Beaudoing, H., Rodell, M., 2018. GLDAS Catchment Land Surface Model L4 daily 0.25 x 0.25 degree V2. 0.
Li, B., et al., 2019. Global GRACE data assimilation for groundwater and drought monitoring: advances and challenges. Water Resour. Res. 55 (9), 7564–7586. https://doi.org/10.1029/2018wr024618.
Li, J., et al., 2020. A new framework for tracking flash drought events in space and time. Catena 194. https://doi.org/10.1016/j.catena.2020.104763.
Li, Z., Chen, Y., Fang, G., Li, Y., 2017. Multivariate assessment and attribution of droughts in Central Asia. Sci. Rep. 7 (1), 1–12.
Lisonbee, J., Woloszyn, M., Skumanich, M., 2021. Making sense of flash drought: definitions, indicators, and where we go from here. J. Appl. Service Climatol. 2021 (1), 1-19. 10.46275/joasc.2021.02.001.
Lloyd-Hughes, B., 2012. A spatio-temporal structure-based approach to drought characterisation. Int. J. Climatol. 32 (3), 406–418. https://doi.org/10.1002/joc.2280.
Lloyd-Hughes, B., 2013. The impracticality of a universal drought definition. Theor. Appl. Climatol. 117 (3–4), 607–611. https://doi.org/10.1007/s00704-013-1025-7.
Martens, B., et al., 2017. GLEAM v3: satellite-based land evaporation and root-zone soil moisture. Geosci. Model Dev. 10 (5), 1903–1925. https://doi.org/10.5194/gmd-10-1903-2017.
McKee, T.B.D., Nolan, J., McKee, J.K., 1993. The relationship of drought frequency and duration to time scales. Eighth Conf. Appl. Climatol. 17.
Miralles, D.G., et al., 2011. Global land-surface evaporation estimated from satellite-based observations. Hydrol. Earth Syst. Sci. 15 (2), 453–469. https://doi.org/10.5194/hess-15-453-2011.
Mishra, A.K., Singh, V.P., 2010. A review of drought concepts. J. Hydrol. 391 (1–2), 202–216. https://doi.org/10.1016/j.jhydrol.2010.07.012.
Mishra, A.K., Singh, V.P., 2011. Drought modeling – A review. J. Hydrol. 403 (1–2), 157–175. https://doi.org/10.1016/j.jhydrol.2011.03.049.
Mo, K.C., Lettenmaier, D.P., 2015. Heat wave flash droughts in decline. Geophys. Res. Lett. 42 (8), 2823–2829. https://doi.org/10.1002/2015gl064018.
Narasimhan, B., Srinivasan, R., 2005. Development and evaluation of Soil Moisture Deficit Index (SMDI) and Evapotranspiration Deficit Index (ETDI) for agricultural drought monitoring. Agric. For. Meteorol. 133 (1–4), 69–88. https://doi.org/10.1016/j.agrformet.2005.07.012.
Nguyen, P., et al., 2019. The CHRS Data Portal, an easily accessible public repository for PERSIANN global satellite precipitation data. Sci. Data 6, 180296. https://doi.org/10.1038/sdata.2018.296.
Nicolai-Shaw, N., Zscheischler, J., Hirschi, M., Gudmundsson, L., Seneviratne, S.I., 2017. A drought event composite analysis using satellite remote-sensing based soil moisture. Remote Sens. Environ. 203, 216–225. https://doi.org/10.1016/j.rse.2017.06.014.
Nicolai-Shaw, N., Gudmundsson, L., Hirschi, M., Seneviratne, S.I., 2016. Long-term predictability of soil moisture dynamics at the global scale: Persistence versus large-scale drivers. Geophys. Res. Lett. 43 (16), 8554–8562. https://doi.org/10.1002/2016gl069847.
Orth, R., Destouni, G., 2018. Drought reduces blue-water fluxes more strongly than green-water fluxes in Europe. Nat. Commun. 9 (1), 3602. https://doi.org/10.1038/s41467-018-06013-7.
Otkin, J.A., et al., 2018. Flash droughts: a review and assessment of the challenges imposed by rapid-onset droughts in the United States. Bull. Am. Meteorol. Soc. 99 (5), 911–919. https://doi.org/10.1175/bams-d-17-0149.1.
Palmer, W.C., 1965. Meteorological Drought, 30. US Department of Commerce, Weather Bureau.
Patrick, E., 2017. Drought characteristics and management in Central Asia and Turkey. FAO Water Reports (FAO). Food and Agriculture Organization of the United Nations Rome, Italy: 114.
Pendergrass, A.G., et al., 2020. Flash droughts present a new challenge for subseasonal-to-seasonal prediction. Nat. Clim. Change 10 (3), 191–199. https://doi.org/10.1038/s41558-020-0709-0.
Rajsekhar, D., Singh, V.P., Mishra, A.K., 2015. Multivariate drought index: An information theory based approach for integrated drought assessment. J. Hydrol. 526, 164–182. https://doi.org/10.1016/j.jhydrol.2014.11.031.
Schober, P., Boer, C., Schwarte, L.A., 2018. Correlation coefficients: appropriate use and interpretation. Anesth Analg 126 (5), 1763–1768. https://doi.org/10.1213/ANE.0000000000002864.
Sheffield, J., Andreadis, K.M., Wood, E.F., Lettenmaier, D.P., 2009. Global and continental drought in the second half of the twentieth century: severity–area–duration analysis and temporal variability of large-scale events. J. Clim. 22 (8), 1962–1981. https://doi.org/10.1175/2008jcli2722.1.
Shukla, S., Wood, A.W., 2008. Use of a standardized runoff index for characterizing hydrologic drought. Geophys. Res. Lett. 35 (2) https://doi.org/10.1029/2007gl032487.
Spinoni, J., et al., 2019. A new global database of meteorological drought events from 1951 to 2016. J Hydrol Reg Stud 22, 100593. https://doi.org/10.1016/j.ejrh.2019.100593.
Stagge, J.H., Tallaksen, L.M., Gudmundsson, L., Van Loon, A.F., Stahl, K., 2015. Candidate distributions for climatological drought indices (SPI and SPEI). Int. J. Climatol. 35 (13), 4027–4040. https://doi.org/10.1002/joc.4267.
Tallaksen, L.M., Hisdal, H., Lanen, H.A.J.V., 2009. Space–time modelling of catchment scale drought characteristics. J. Hydrol. 375 (3–4), 363–372. https://doi.org/10.1016/j.jhydrol.2009.06.032.
Taylor, R., 1990. Interpretation of the correlation coefficient: a basic review. J. Diagn. Med. Sonogr. 6 (1), 35–39.
Trambauer, P., Maskey, S., Winsemius, H., Werner, M., Uhlenbrook, S., 2013. A review of continental scale hydrological models and their suitability for drought forecasting in (sub-Saharan) Africa. Phys. Chem. Earth, Parts A/B/C 66, 16–26. https://doi.org/10.1016/j.pce.2013.07.003.
Van Loon, A.F., 2015. Hydrological drought explained. Wiley Interdisciplinary Rev.: Water 2 (4), 359–392. https://doi.org/10.1002/wat2.1085.
Van Loon, A.F., Van Huijgevoort, M.H.J., Van Lanen, H.A.J., 2012. Evaluation of drought propagation in an ensemble mean of large-scale hydrological models. Hydrol. Earth Syst. Sci. 16 (11), 4057–4078. https://doi.org/10.5194/hess-16-4057-2012.
Van Loon, A.F., Van Lanen, H.A.J., 2012. A process-based typology of hydrological drought. Hydrol. Earth Syst. Sci. 16 (7), 1915–1946. https://doi.org/10.5194/hess-16-1915-2012.
Vicente-Serrano, S.M., et al., 2018. Global assessment of the standardized evapotranspiration deficit index (SEDI) for drought analysis and monitoring. J. Clim. 31 (14), 5371–5393. https://doi.org/10.1175/jcli-d-17-0775.1.
Wang, A., Lettenmaier, D.P., Sheffield, J., 2011. Soil moisture drought in China, 1950–2006. J. Clim. 24 (13), 3257–3271. https://doi.org/10.1175/2011jcli3733.1.
Wang, W., Ertsen, M.W., Svoboda, M.D., Hafeez, M., 2016. Propagation of drought: from meteorological drought to agricultural and hydrological drought. Adv. Meteorol. 2016, 1–5. https://doi.org/10.1155/2016/6547209.
Wu, J., Chen, X., Yao, H., Zhang, D., 2021. Multi-timescale assessment of propagation thresholds from meteorological to hydrological drought. Sci. Total Environ. 765, 144232 https://doi.org/10.1016/j.scitotenv.2020.144232.
Wu, J., et al., 2018. Meteorological and Hydrological Drought on the Loess Plateau, China: Evolutionary Characteristics, Impact, and Propagation. Journal of Geophysical Research: Atmospheres 123 (20), 11569–11584. https://doi.org/10.1029/2018jd029145.
Xu, Y., et al., 2019. Propagation from meteorological drought to hydrological drought under the impact of human activities: a case study in northern China. J. Hydrol. 579 https://doi.org/10.1016/j.jhydrol.2019.124147.
Yang, H., Mu, S., Li, J., 2014. Effects of ecological restoration projects on land use and land cover change and its influences on territorial NPP in Xinjiang, China. Catena 115, 85–95. https://doi.org/10.1016/j.catena.2013.11.020.
Yevjevich, V., 1967. An objective approach to definitions and investigations of continental hydrologic droughts. Hydrology Papers.
Zargar, A.S., Rehan; Naser, Bahman; Khan, Faisal, 2011. A review of drought indices. Environ. Rev. (19): 333-349. https://doi.org/10.1139/a11-013.
Zhu, Y., Wang, W., Singh, V.P., Liu, Y., 2016. Combined use of meteorological drought indices at multi-time scales for improving hydrological drought detection. Sci. Total Environ. 571, 1058–1068. https://doi.org/10.1016/j.scitotenv.2016.07.096.